Cancer Chemother Pharmacol (1999) 44: 1–11

ORIGINAL ARTICLE

**Mary Jane Elliott · Kathleen M. Murphy
Lolita Stribinskiene · Velvizhi Ranganathan
Eric Sturges · Monica L. Farnsworth · Richard B. Lock**

Bcl-2 inhibits early apoptotic events and reveals post-mitotic multinucleation without affecting cell cycle arrest in human epithelial tumor cells exposed to etoposide

Received: 1 September 1998 / Accepted: 3 November 1998

Abstract Defective apoptotic mechanisms are considered to play a role in both the development of malignancy and resistance to chemotherapeutic drugs. The Bcl-2 family of proteins regulate the cellular commitment to survive or die when challenged with various apoptotic stimuli. *Purpose*: The purpose of this study was to identify the point at which Bcl-2 interrupts the apoptotic cascade initiated following exposure of human tumor cells to etoposide. *Methods*: A stable Bcl-2-expressing HeLa-transfected clonal cell line, along with its control-vector-transfected counterpart, were utilized in this study. Following etoposide exposure, cells were examined for cell cycle arrest, formation of hyperdiploid cells, apoptotic DNA degradation, loss of plasma membrane integrity, levels of expression of members of the Bcl-2 protein family, caspase activation, degradation of poly(ADP-ribose) polymerase and movement of Bax from cytosol to cellular membrane fractions. *Results*: Caspase activation, poly(ADP-ribose) polymerase degradation and Bax membrane insertion were initiated rapidly following etoposide removal, concomitantly with cell cycle arrest. Whereas Bcl-2 had no effect on etoposide-induced cell arrest, it interrupted all aspects of apoptosis, including activation of caspases, poly(ADP-ribose) polymerase degradation, DNA fragmentation and loss of plasma membrane integrity. Surprisingly, Bcl-2 also blocked Bax membrane insertion. In addition, Bcl-2 also prevented the increase in cellular levels of Bak, Bax and Bcl-x_L, along with degradation of actin and Bax. However, inhibition of etoposide-induced apoptosis by Bcl-2 resulted in the accumulation of giant, multinucleated cells that eventually lost the ability to exclude trypan blue without apoptotic morphology or DNA degradation. *Conclusions*: These results indicate that biochemical apoptotic processes are initiated concomitant with etoposide-induced cell cycle arrest and are interrupted by Bcl-2 overexpression. However, the aberrant mitotic events induced by etoposide are sufficient to kill these cells even in the absence of apoptosis.

Key words Apoptosis · Bax · Bcl-2 · Cell cycle check-points · Etoposide

Abbreviations *Ac-DEVD-pNa N*-Acetyl-Asp-Glu-Val-Asp-*p*-nitroanilide · *PARP* Poly(ADP-ribose) polymerase · *PBS* Calcium- and magnesium-free phosphate-buffered saline

Introduction

Despite tremendous advances in our understanding of the mechanisms by which cancer develops, the major barrier to its eradication with chemotherapy remains drug resistance. Delineating the mechanisms of drug resistance will allow the design of treatment strategies aimed at their circumvention, leading to improved patient survival rates and quality of life. Studies carried out over the last 30 years have focused upon how tumor cells evade death by developing mechanisms that prevent drugs from interacting with their cellular targets. However, recent discoveries indicate that tumor cells may express defects in a programmed-cell-death mechanism (apoptosis) that makes them resistant to chemotherapy, regardless of the agent to which they are exposed

M.J. Elliott · L. Stribinskiene · V. Ranganathan · E. Sturges
The Henry Vogt Cancer Research Institute,
J. Graham Brown Cancer Center,
Department of Medicine and Department of Biochemistry and Molecular Biology, University of Louisville,
Louisville, KY 40202, USA

K.M. Murphy
Department of Microbiology and Immunology,
University of Louisville,
Louisville, KY 40202, USA

M.L. Farnsworth · R.B. Lock (✉)
Children's Cancer Research Institute,
University of New South Wales, Sydney Children's Hospital,
Randwick, Sydney 2031, Australia
Tel.: +61-2-9382-1822; Fax: +61-2-9382-1850
e-mail: Richard.Lock@unsw.edu.au

[1, 18, 38, 46]. These discoveries have had a significant impact upon our perception not only of anticancer drug resistance but also of the nature in which cancer can develop. For these reasons and because apoptosis is a significant pathway by which chemotherapeutic drugs eliminate target cells [17, 26], a tremendous effort has been mounted to delineate the molecular mechanisms of anticancer drug-induced apoptosis.

Apoptosis, in which a cell actively participates in its own demise, was originally characterized morphologically by cell shrinkage, plasma membrane blebbing, condensation of chromatin around the nuclear periphery, and cell disintegration into plasma membrane-bound apoptotic bodies [25]. Recent data indicate that all of these processes are controlled by a sequential cascade of activation, by proteolytic cleavage, of a family of *c*ysteine-dependent, *asp*artate-specific prote*ases* (caspases) [7, 13, 39]. Different members of the caspase family exhibit variations in substrate sequence requirements N-terminally to the required aspartate residue [7, 52]. For example, caspase-3 (also known as CPP32/YAMA/apopain) preferentially cleaves on the carboxyl side of the tetrapeptide sequence Asp-Glu-Val-Asp (DEVD), a sequence present in PARP [30]. Indeed, cleavage of PARP is considered an early marker for chemotherapeutic drug-induced apoptosis [7, 24, 57]. Proteolysis of the 113-kDa PARP protein by caspase-3 generates 89- and 24-kDa cleavage products [44]. Additional proteins that serve as targets for the caspase family include nuclear lamins, DNA-activated protein kinase, actin, U1-70-kDa protein, and protein kinase Cδ [7, 11, 47]. Activation of caspase-3, which may serve as a convergence point for differing apoptotic stimuli [7, 39, 47], is catalyzed in vitro by cleavage of pro-caspase-3 by caspase-9 [31]. Activation of pro-caspase-9 itself through catalytic cleavage is controlled by a complex of Apaf-1 (the human homolog of the *Caenorhabditis elegans* CED-4 protein), cytochrome c and dATP [31]. Caspase activity in cell lysates can be conveniently monitored by cleavage of chromogenic of fluorogenic tetrapeptide substrates [7, 52].

The epipodophyllotoxin etoposide exerts its cell-killing effects through DNA damage mediated by the nuclear enzyme DNA topoisomerase II [6]. At non-supralethal concentrations, etoposide induces G2 arrest [8, 32, 34, 36, 41], which may or may not be followed by apoptotic death [35, 36, 41]. Activation of multiple caspases and cleavage of PARP have been documented extensively in etoposide-induced apoptosis of human tumor cells [12, 24, 40, 41, 43, 54, 57]. However, with the exception of the recent report by Martins et al. [41], morphological evidence of apoptosis was induced within 6 h of drug exposure.

The Bcl-2 family of proteins appear to interact to regulate the commitment to survive or die on challenge with various apoptotic stimuli by controlling the flux of ions and proteins through intracellular membranes [56]. Pro-apoptotic members of the family include Bax, Bak and Bcl-x_S, whereas anti-apoptotic members include Bcl-2, Bcl-x_L and Bcl-w [29]. Bax has recently been shown to induce the release of cytochrome c (with the ensuing caspase-3 activation and apoptosis) from mitochondria [23, 48], whereas Bcl-2 and Bcl-x_L can interfere with caspase activation at the point of cytochrome c release or downstream thereof [2, 28, 31, 48, 57]. Furthermore, it has been demonstrated that Bax is an almost exclusively cytosolic protein that translocates to cytoplasmic membranes upon exposure of cells to an apoptotic stress such as the protein kinase inhibitor staurosporine [22, 55]. This observation challenges the dogma that Bcl-2 (which is restricted to cellular membrane compartments) and Bax form heterodimers in cells not exposed to an apoptosis-inducing stress. Indeed, the degree of interaction between pro- and anti-apoptotic members of the Bcl-2 family that is detected by immunoprecipitation assays may be an artefact of detergent cell lysis [20, 21].

We have developed a model system to study the sole contribution of Bcl-2 to drug resistance of human epithelial tumor (HeLa) cells, whereby significant levels of morphologically apoptotic cells are not detected until after the manifestation of etoposide-induced G2 arrest [35]. Whereas Bcl-2 was capable of inhibiting etoposide-induced apoptosis, it could not enhance clonogenic survival, due to post-mitotic catastrophe multinucleation [35]. More recently we have reported that Bcl-2 can enhance clonogenic survival in a drug-specific fashion in these cells [10]. In the present report we utilize this model system to relate temporally etoposide-induced G2 arrest to caspase activation and the initiation of additional apoptotic events with respect to the point of inhibition by Bcl-2. Our data indicate that Bcl-2 does not affect G2 arrest but prevents caspase activation and PARP cleavage, which are early events occurring in concert with Bax subcellular redistribution. Inhibition of apoptosis by Bcl-2 results in the accumulation of terminally G2-arrested or multinucleated cells that eventually lose plasma membrane integrity. Furthermore, apparent changes in intracellular levels of Bax, Bak and Bcl-x_L following etoposide treatment are prevented by Bcl-2 overexpression, indicating that they are sequelae of the apoptotic process.

Materials and methods

Reagents and cell lines

All reagents and their sources have been detailed in previous publications [10, 35]. The transfection, selection and growth conditions used for both the control-vector-transfected (S-1) and the stable Bcl-2 expressing (B-5) HeLa clones used in this study have also been described elsewhere [10, 35].

Cell viability, cytology techniques and cell cycle analysis

Exponentially dividing cells were exposed to etoposide, following which they were washed twice with 37 °C PBS and incubated in drug-free medium. At the appropriate time points, cells were harvested and viability was estimated as the proportion of cells that excluded 0.2% trypan blue [10, 35]. For morphological

determination of the proportion of apoptotic and multinucleated cells, 15,000 cells were spun onto a microscope slide and stained with Wright/Giemsa stains [10, 35, 36]. In all, 1,000 cells were counted and scored as either normal, multinucleated (large, multiple nuclei) or apoptotic (condensed, intense chromatin staining) as reported previously [10, 35, 36].

For cell cycle analysis, cell suspensions were washed twice in ice-cold PBS, fixed in 70% cold ethanol and stored at −20 °C until all time points were collected. Samples were then washed twice in ice-cold PBS and resuspended in 500 µl of PBS containing propidium iodide at 5 µg/ml and RNase A at 500 µg/ml. Following a 20-min period of incubation at room temperature in darkness, flow cytometric analysis was performed using a FACscan (Becton-Dickinson). Data were analyzed using the CellFit Cell-Cycle Analysis program (Version 2.01.2).

Flow cytometric differentiation between apoptotic and multinucleated cells

Analysis of apoptotic DNA fragmentation was performed using end-labelling of nicked DNA with biotin-conjugated dUTP by terminal deoxynucleotidyl transferase (TdT) [14]. Single-cell suspensions were fixed with 1% paraformaldehyde in PBS for 15 min on ice, washed in ice-cold PBS, fixed in 70% ethanol and stored at −20 °C until all time points were harvested. Altogether, 2 million cells/sample were centrifuged, washed twice with ice-cold PBS and resuspended in 50 µl of enzyme buffer containing 1 m*M* $CoCl_2$, 0.5 nmol of biotin-dUTP and 10 U of Tdt (Boehringer Mannheim Biochemicals). Following a 30-min period of incubation at 37 °C, cells were washed in PBS and resuspended in 100 µl of fluorescein isothiocyanate (FITC) staining solution [fluoresceinated avidin at 2.5 µg/ml, 4 × SSC, 0.1% Triton X-100 and 5% (w/v) non-fat dry milk] [14]. After 30 min of incubation at room temperature in darkness, cells were washed twice with PBS and resuspended in propidium iodide/RNase solution as described for cell cycle analysis above. The percentages of cells in each phase of the cell cycle, those that were apoptotic and those that were hyperdiploid were assessed by dual-color flow cytometric analysis using a Coulter Elite flow cytometer, and the analysis was gated to exclude cell doublets. For each experiment, gates were drawn manually for quantitation of the proportion of apoptotic, hyperdiploid and G1/S/G2/M cell populations. Gates remained fixed during the course of each experiment.

Immunoblotting procedures

For the detection of Bcl-2, Bax, Bak and Bcl-X proteins, cell extracts were prepared by lysis of cells in PBS containing 1% NP-40 as described previously [35, 37]. For PARP immunoblots, cells were lysed in RIPA buffer [50 m*M* TRIS-Cl (pH 7.5), 150 m*M* NaCl, 1% NP-40, 0.5% sodium deoxycholate, 0.1% sodium dodecyl sulfate (SDS), 50 m*M* sodium fluoride, 0.1 m*M* sodium orthovanadate] containing a protease-inhibitor cocktail [35, 37]. Protein concentration was estimated by the bicinchoninic acid assay method (Pierce) using bovine serum albumin (BSA) as the standard. Equal loading and transfer of proteins to polyvinylidene difluoride membranes following SDS-polyacrylamide gel electrophoresis (PAGE) was verified by staining of each membrane with Ponceau S prior to blocking of non-specific binding sites. Immunoblotting was carried out as described previously [32, 33, 35] using antihuman Bcl-2, Bax, Bak and Bcl-X polyclonal antisera (PharMingen), an anti-actin polyclonal antibody (Sigma), an anti-PARP monoclonal antibody (clone C-2-10, Novus Molecular), and the antihuman topoisomerase I monoclonal antibody (clone C-21, kindly provided by Dr. Y.-C. Cheng, Yale University School of Medicine, New Haven, Conn., USA). Chemiluminescent signals were quantified using Hyperfilm MP (Amersham) that had been brought to the linear response range by preflashing to an OD_{540} of 0.15. The intensity of each protein band was quantified using NIH Image software after scanning of the image using a MicroTek ScanMaker III equipped with a transparency adaptor. PARP degradation was expressed as the percentage of the 113-kDa protein that proteolyzed to the 89-kDa fragment [44].

Caspase activity assays

Cells were harvested, washed twice with ice-cold PBS, and lysed by six freeze/thaw cycles in 50 m*M* PIPES (pH 7.4), 50 m*M* KCl, 5 m*M* $MgCl_2$, 5 m*M* ethylene glycol tetraacetic acid (EGTA), 1 m*M* phenylmethylsulfonylfluoride (PMSF), pepstatin A at 10 µg/ml, and leupeptin at 10 µg/ml at a density of 10^8 cells/ml. The lysate was centrifuged at 10,000 *g* for 10 min at 4 °C and the supernatant was used to estimate caspase activity by cleavage of the synthetic CPP32 (caspase-3) substrate Ac-DEVD-pNA. The equivalent of 100 µg of protein from cell lysates was pipetted into each well of a 96-well plate, and 100 µl of reaction buffer [20 m*M* PIPES (pH 7.2), 100 m*M* NaCl, 10% sucrose, 0.1% CHAPS, 20 m*M* 2-mercaptoethanol] containing peptide substrate (final concentration 100 µ*M*) was added. Following 1 h of incubation at 37 °C the absorbance recorded at 405 nm (A_{405}) was subtracted from that noted in each well at time zero. The Ac-DEVD-pNa cleavage activity was expressed as A_{405} per hour per milligram of cellular protein. Preliminary experiments had verified the linearity of the response over time and protein concentration (data not shown).

Subcellular fractionation

For separation of subcellular cytosolic and nuclear/membrane fractions, 10 million cells were washed twice with ice-cold PBS, resuspended in 1 ml of hypotonic lysis buffer [10 m*M* HEPES (pH 7.4), 10 m*M* NaCl, PMSF at 25 µg/ml, leupeptin at 1 µg/ml, and aprotinin at 1 µg/ml] and incubated on ice for 30 min. The cells were then disrupted by six to seven cycles of freezing in liquid nitrogen and thawing at 37 °C. After microscopic verification that >95% of the cells had lysed the crude lysate was subjected to centrifugation at 100,000 *g* for 1 h at 4 °C. The resultant supernatant, which consisted of the cytosol, was separated from the pellet, which represented the cellular membrane, organelle, and nuclear fractions. The pellet was resuspended in 1 ml of hypotonic buffer. Equal volumes of cytosolic and membrane fractions were separated by SDS-PAGE, transferred to polyvinylidene difluoride membranes and immunoblotted using Bax, Bcl-2 and actin polyclonal antisera. The extent of cross-contamination of each fraction was verified by measurement of the activity of lactate dehydrogenase (a cytosolic marker) followed by immunoblotting for the nuclear protein topoisomerase I. Experiments were deemed valid only if >95% of the total lactate dehydrogenase activity and 100% of the topoisomerase I protein appeared in the cytosolic and membrane fractions, respectively.

Statistics

Unless stated otherwise, numerical data represent mean values for at least two experiments. Standard errors, unless shown, were generally less than 15% of the value of the respective data point.

Results

We previously demonstrated that Bcl-2 overexpression in HeLa cells substantially delayed or inhibited the onset of apoptosis and loss of plasma membrane integrity following etoposide exposure without enhancing clonogenic survival [35]. The Bcl-2-expressing cells (B-5) did not exhibit a significant difference in population-doubling time as compared with control-vector-transfected

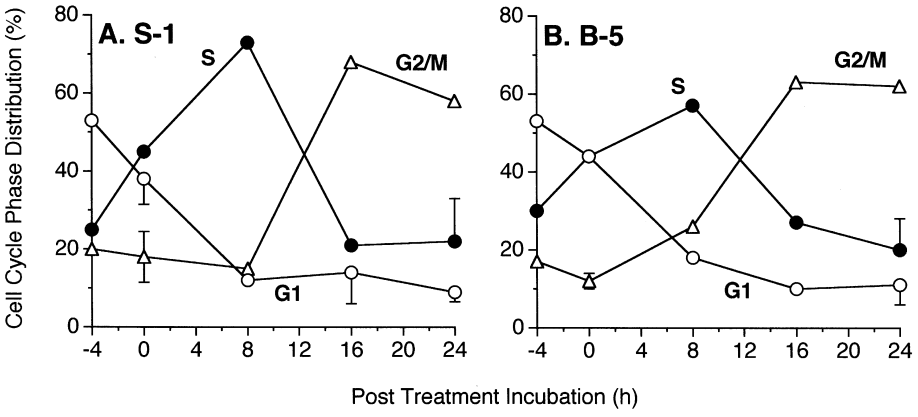

Fig. 1A,B Bcl-2 overexpression has no significant effect on cell cycle distribution of HeLa cells following etoposide treatment. **A** HeLa S-1 or **B** B-5 cells were exposed to etoposide (25 μ*M*, 4 h) and harvested for cell cycle analysis at various time points thereafter. The proportions of G1-(*white circles*), S-(*black circles*) and G2/M-phase cells (*white triangles*) were individually estimated as a percentage of the total (10,000) events. Data represent mean values for two separate experiments

cells (S-1) [35]. In addition, the colony-forming efficiency of these two clones were comparable (50.5 ± 3.6% and 49.2 ± 4.4% for S-1 and B-5 cells, respectively; $n = 4$). We wished to explore further the discrepancy between induction of cell death and inhibition of clonogenic survival in these Bcl-2-expressing cells by monitoring varous parameters of cell cycle progression and apoptosis following etoposide treatment. Exposure of B-5 or S-1 cells to etoposide resulted in a transient delay in the S phase, which was followed by the accumulation of 60–70% of cells in the G2/M phase (Fig. 1). Within the initial 24 h following drug removal, Bcl-2 expression exerted no significant effect on the cell-cycle arrest characteristics of HeLa cells exposed to etoposide.

Bcl-2 expression in HeLa cells has been shown to allow the accumulation of giant, multinucleated (>4n, hyperdiploid) cells following exposure to etoposide by preventing apoptosis [35]. A flow cytometry technique was utilized to discriminate G1-, S- and G2/M-phase cells from those that were either >4n (hyperdiploid) or apoptotic (Fig. 2). In Fig. 2 the amount of biotin-dUTP that was incorporated into cellular DNA in the presence of Tdt is plotted on the abscissa (FITC), whereas the DNA content per cell is plotted on the ordinate (PI). G1, S and G2/M cells are represented in region 1; hyperdiploid or multinucleated (>4n) cells are contained in region 2; and apoptotic cells appear in region 3 (Tdt-positive). Control populations of S-1 and B-5 cells exhibited >95% of events in the "normal" G1, S and G2/M region (region 1 in Fig. 2A, C). However, at 6 days after etoposide treatment, >80% of events in the S-1 population appeared in region 3 (apoptotic, Fig. 2B), whereas <10% of B-5 events were in this region (Fig. 2D). In contrast, etoposide-treated B-5 cells appeared as approximately equal proportions of terminally G2-arrested or hyperdiploid events (Fig. 2D, regions 1 and 2, respectively). The representative cell morphology is shown in the inset of each plot. Thus, it would appear that terminally G2-arrested or hyperdiploid HeLa cells undergo apoptosis and that this can be inhibited by ectopic Bcl-2 expression.

The progression of etoposide-treated S-1 and B-5 HeLa cells into G2 delay, a hyperdiploid state, and apoptosis is represented quantitatively in Fig. 3. In addition, Fig. 3 shows the loss of viability as demonstrated by the plasma-membrane-integrity assay of trypan blue exclusion. Control S-1 and B-5 populations contained only approximately 20% G2/M cells, with very few hyperdiploid or apoptotic cells and the remainder of cells were in the G1 or S phase (see Fig. 1). In the S-1 cells, significant loss of viability occurred in parallel with the emergence of Tdt-positive (apoptotic) cells and following the appearance of G2-arrested and hyperdiploid cells (Fig. 3A). In contrast, >90% of B-5 cells exposed to etoposide remained either terminally G2-arrested or became hyperdiploid over the 6-day incubation period, without a high proportion of apoptotic cells being detected (Fig. 3B), despite the observation that B-5 cells gradually lost plasma membrane integrity. Therefore, the loss of plasma membrane integrity in B-5 cells cannot be attributed to apoptosis alone, unlike the situation in S-1 cells (Fig. 3, cf. A and B), indicating that Bcl-2 overexpression has redirected at least half of the cells through an alternative death pathway. During extended time-course experiments, B-5 cells did not exhibit a greater tendency that S-1 cells to recover and repopulate culture dishes following etoposide exposure (data not shown).

The S-1 and B-5 clones represent a useful model system for the study of drug-induced mechanisms of apoptosis in human epithelial tumor cells, in which the triggering events can be separated from the sequelae of apoptosis. Due to the ability of Bcl-2 to inhibit etoposide-induced apoptosis in HeLa cells, it was reasoned that the pro-apoptotic members of the Bcl-2 family (such as Bax and Bak) might be involved in the apoptosis-triggering events. Furthermore, we wished to determine whether the inhibitory effects of Bcl-2 occurred via direct interactions with Bax and Bak proteins.

Experiments were performed to estimate intracellular levels of Bcl-2 family members in etoposide-treated cells (Fig. 4). Figure 4A shows representative immunoblots, whereas each data point in Fig. 4B and Fig. 4C represents the mean value for three separate experiments. The earliest change detected in this set of experiments was a significant increase in Bak protein levels in S-1 cells at 1 day following etoposide removal (Fig. 4A,B). Bak levels

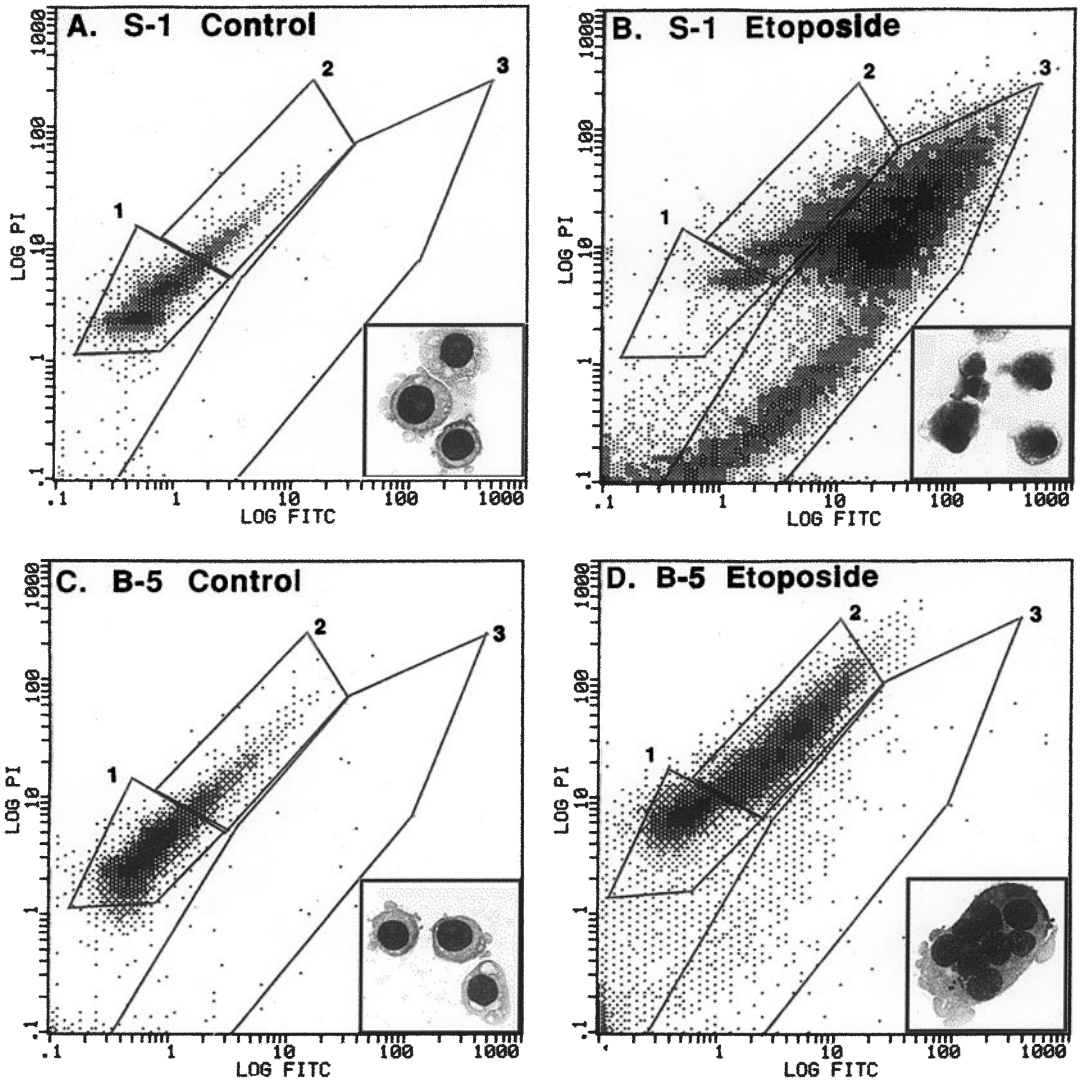

Fig. 2A–D Flow cytometric separation of normal, hyperdiploid, and apoptotic cells. Following etoposide treatment (25 μ*M*, 4 h), cells were harvested, prepared for cell cycle and Tdt ananlysis, and processed by flow cytometry as described in Materials and methods. Manual gates were drawn around the G1, S and G2/M ("normal", *region 1*), the hyperdiploid (FITC-dim, *region 2*), and the apoptotic (FITC-bright, *region 3*) cell populations. Each histogram is representative of at least three separate experiments and shows **A, B** S-1 or **C, D** B-5 cells exposed to either **A, C** solvent control or **B, D** etoposide and harvested 6 days post treatment. The representative cell morphology is shown as an *inset* in each histogram

continued to increase during the overall time course. In addition, Bax and (paradoxically) Bcl-x_L levels began to increase at 2 days following etoposide removal in S-1 cells and continued to increase throughout the time course. The increase in Bax levels was accompanied by its degradation to lower-molecular-weight species, with over 40% being degraded at 6 days post treatment (Fig. 4A). Finally, actin levels began to decline noticeably in S-1 cells at 4 days following the removal of etoposide. Further experimentation confirmed that no change in the intracellular concentration of these proteins occurred prior to the 24-h time point (data not shown).

In contrast, levels of Bak, Bax, Bcl-x_L and actin did not change significantly in etoposide-treated B-5 cells over the time course studied (Fig. 4A,C). These data indicate that the changes in the levels of all four proteins observed in S-1 cells can be inhibited by Bcl-2 overexpression (in B-5 cells). Furthermore, these changes are not due to etoposide-induced cell cycle arrest, which did not differ in S-1 and B-5 cells, and likely occur downstream of the point at which Bcl-2 acts to prevent apoptosis.

The Bcl-2 protein was not detected in S-1 cells and its expression was not significantly altered in etoposide-treated B-5 cells, whereas the Bcl-x_S protein (resulting from an alternatively-spliced form of the Bcl-X mRNA) was not detected in S-1 or B-5 cells (data not shown).

Cleavage of the nuclear enzyme PARP by caspase-3 has been proposed as an early event in chemotherapeutic drug-induced apoptosis [7, 24, 57]. Therefore, we wished to relate temporally PARP cleavage and caspase activity in etoposide-treated HeLa cells to the observations

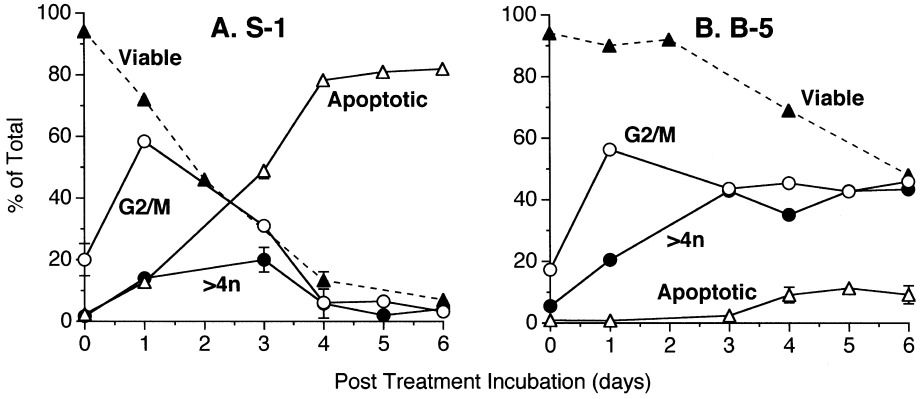

Fig. 3A,B Inhibition of etoposide-induced apoptosis by Bcl-2 results in the accumulation of terminally G2-arrested or hyperdiploid cells. **A** S-1 and **B** B-5 cells were exposed to etoposide (25 μM, 4 h) and harvested at various time points following removal of the drug. Viability was estimated by the exclusion of 0.2% trypan blue, and the remainder of cells were processed for flow cytometric analysis of G2/M, hyperdiploid (>4n) and apoptotic cells as described for Fig. 2. The number of events in each gated region is plotted as a percentage of the total events in regions 1, 2 and 3 shown in Fig. 2 (10,000 events). Data points represent mean values for at least two separate experiments

described above, in which appreciable levels of apoptosis are not detected until after the manifestation of G2 arrest and multinucleation. PARP cleavage was estimated by immunoblotting, whereas caspase activity in cell lysates was monitored by cleavage of the chromogenic substrate Ac-DEVD-pNA. Significant levels of the 89-kDa PARP cleavage product were present within 8 h of the removal of etoposide from S-1 cells (Fig. 5A,B), with over 75% being degraded by 16 h. Similarly, the caspase activity in S-1 cells was observed to increase within 8 h of drug removal, with a continued increase being noted at 16 and 24 h (Fig. 5A). This increase was accompanied by a decrease in and the ultimate disappearance of the 32-kDa form of pro-caspase-3 (CPP32) as detected by immunoblotting (data not shown). In contrast, caspase activity and PARP degradation were not detected in B-5 cells until at least 48 h post treatment (Fig. 5B; data not shown).

During the course of these experiments we were incapable of detecting cleavage activities against a caspase-1 synthetic substrate (Ac-YVAD-pNA) or a substrate corresponding to the caspase cleavage site on protein kinase Cδ (Ac-DMQD-pNA) in etoposide-treated S-1 or B-5 cells (data not shown) [7, 52].

Considerable data have accumulated to support the model that Bax initiates caspase activation by translocating from the cytosol to mitochondrial subcellular compartments, thereby facilitating the release of cytochrome c [22, 23, 48, 55]. To relate temporally this Bax membrane insertion event to our observations of apoptosis in HeLa cells, subcellular fractionation procedures were performed on etoposide-treated S-1 and B-5 cells. Less than 10% of total cellular Bax was present in the insoluble membrane fraction of non-drug-treated S-1

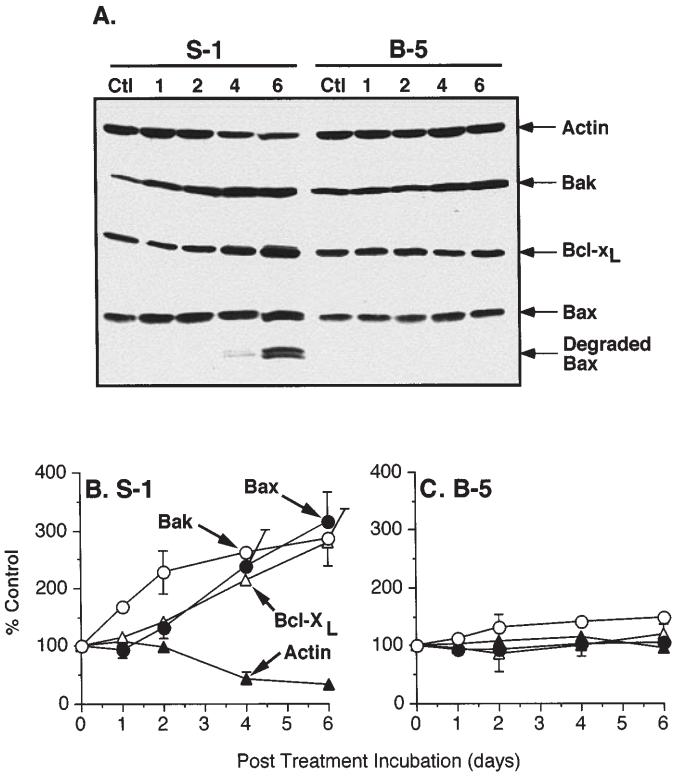

Fig. 4A–C Immunoblot analysis of intracellular levels of Bcl-2 protein family members in etoposide-treated **A, B** S-1 and **A, C** B-5 cells. Cells were exposed to etoposide as described in the legends to Figs. 1–3 and harvested for immunoblot analysis at various days thereafter. Immunoblot analysis was performed as described in Materials and methods. **A** Blot representative of at least three separate experiments; the *integers above each lane* denote the number of days following etoposide removal (*Ctl* Solvent-treated control). **B, C** Mean relative levels of each protein determined as a percentage of solvent-treated controls over three separate experiments. Each graph depicts the relative levels of Bak (*white circles*), Bax (*black circles*), Bcl-x_L (*white triangles*) and actin (*black triangles*)

and B-5 cells (Fig. 5A,C; lanes 2, 6). However, the proportion of membrane-associated Bax significantly increased in S-1 cells within 8 h of etoposide removal, in concert with caspase activation and PARP degradation (Fig. 5A), and continued to rise over the 24-h time course (Fig. 5A,C; cf. lanes 2 and 4). At 72 h following

etoposide removal, <20% of Bax remained in the cytosol (data not shown). In contrast, Bax subcellular relocalisation was not observed in etoposide-treated B-5 cells (Fig. 5C, cf. lanes 6 and 8; data not shown), indicating that Bcl-2 overexpression inhibits the Bax membrane insertion event. Thus, a relatively early event in etoposide-induced apoptosis in HeLa cells is Bax translocation from the cytosol to the insoluble cellular compartments, and this can be inhibited by Bcl-2 overexpression. In these experiments, over 90% of Bax (cytosolic fraction) and 100% of Bcl-2 (membrane/organelle/nuclear fraction) were localized to separate subcellular compartments in B-5 cells (Fig. 5C), which calls into question their ability to heterodimerize in cells not subjected to an apoptosis-inducing stress. Approximately 90% of actin appeared in the cytosolic fractions of S-1 and B-5 cells, regardless of etoposide exposure (Fig. 5C).

The distribution of Bcl-x_L, which was approximately equal between cytosolic and membrane fractions in non-treated cells (F ig. 5C; lanes 1, 2, 5, 6), exhibited a slight shift towards the membrane fraction following etoposide teatment of S-1 cells (lanes 3, 4). Similar to the case of Bax, this shift in distribution was inhibited by Bcl-2 overexpression (lanes 7, 8).

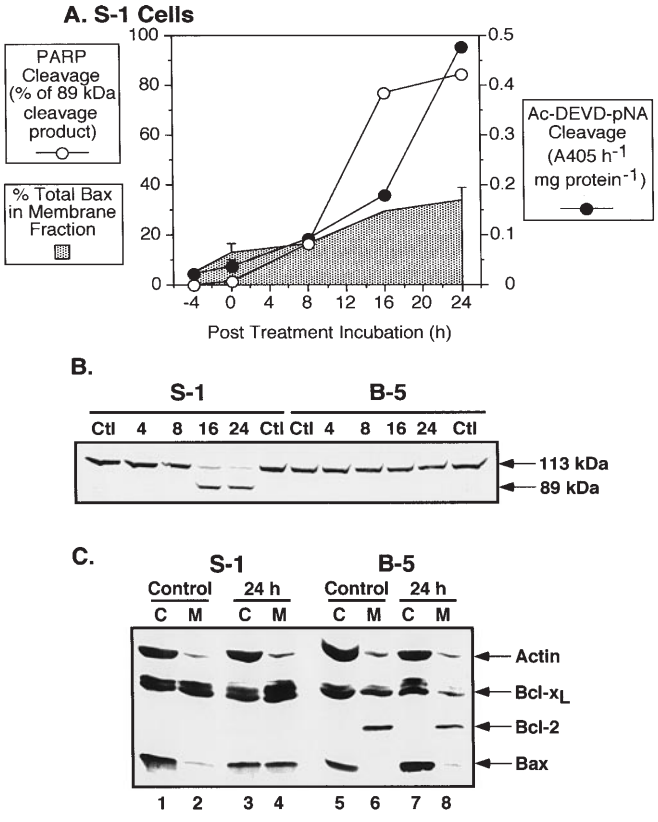

Fig. 5A–C Analysis and quantitation of apoptotic events in etoposide-treated S-1 and B-5 cells. Cells were exposed to etoposide (25 μ*M*, 4 h) and harvested at appropriate time points for immunoblot analysis, subcellular fractionation, or estimation of DEVD-specific cleavage activity as described in Materials and methods. **A** PARP degradation (*white circles*), DEVD-specific cleavage activity (*black circles*), and the proportion of Bax protein in the cellular membrane fraction (*shaded area*) of S-1 cells. Data represent mean values for two separate experiments. **B, C** Representative immunoblots of **B** PARP cleavage and **C** Bax subcellular distribution. **B** The *integers above each lane* denote the number of hours following etoposide removal (*Ctl,* Solvent-treated controls) **C** S-1 (*lanes 1–4*) and B-5 (*lanes 5–8*) cells were exposed to solvent control (*lanes 1, 2, 5, 6*) or harvested 24 h following etoposide removal (*lanes 3, 4, 7, 8*). Cells were fractionated into cytosolic (*C, lanes 1, 3, 5, 7*) or insoluble membrane (*M, lanes 2, 4, 6, 8*) fractions and analyzed by immunoblotting

Discussion

In this report we have attempted to relate temporally apoptotic events and their inhibition by Bcl-2 in human tumor cells exposed to a concentration of etoposide that does not induce appreciable levels of morphological cell death until after the manifestation of G2 arrest. The majority of previous studies have used etoposide to induce apoptosis within 6 h [12, 24, 40, 41, 43, 54, 57]. The salient findings of the present study are that (a) caspase activation, PARP cleavage and Bax membrane insertion are early events in etoposide-induced apoptosis of HeLa cells and occur concomitantly with cell cycle arrest; (b) Bcl-2 overexpression, while not affecting etoposide-induced cell-cycle arrest, inhibits or substantially delays Bax membrane insertion, caspase activation, PARP degradation and the subsequent manifestations of apoptosis, including DNA fragmentation and loss of plasma membrane integrity; (c) the increase in cellular levels of Bax, Bak and Bcl-x_L proteins following etoposide treatment do not occur in the context of Bcl-2 overexpression and, therefore, are sequelae of the apoptotic process; and (d) inhibition of etoposide-induced apoptosis by Bcl-2 results in the accumulation of terminally G2-arrested or multinucleated cells that eventually lose their ability to preserve plasma membrane integrity.

The temporal relationships between etoposide-induced apoptotic events in HeLa cells described in this report are in general agreement with the overall model for apoptosis caused by etoposide in several model systems [12, 24, 40, 41, 43, 54, 57]. However, our report contributes the additional observations that Bax membrane insertion, induction of DEVD-specific cleavage activity, and PARP degradation are relatively early events in HeLa cells and occur concomitantly with rather than subsequently to cell cycle arrest. It was recently demonstrated that Bax relocated from the cytosol to mitochondria during staurosporine-induced apoptosis and that removal of the C-terminal transmembrane domain of Bax prevented both Bax insertion and apoptosis [55]. Presumably, Bax membrane insertion in etoposide-treated HeLa cells causes mitochondrial release of cytochrome c, which precedes caspase activation and amplification of the apoptotic cascade [48]. However, we could not temporally separate the events of Bax membrane insertion, caspase activation and PARP cleavage in these cells, which appear to occur simultaneously (Fig. 5A). Similarly, we could not temporally

separate these events in staurosporine-treated HeLa, HL60 (human promyelogenous leukemia) and MCF10A (human normal breast epithelial) cells (data not shown). Additional experimentation is required to delineate the dependent relationships between Bax membrane insertion and caspase activation in drug-induced cell death.

Preliminary immunofluorescence examination indicates that the Bax movement from the cytosol to membrane fractions in subcellular fractionation experiments is due to mitochondrial localization rather than to the endoplasmic reticulum or nucleus (data not shown). In addition, it is likely that the DEVD cleavage activity detected in lysates from etoposide-treated HeLa cells is contributed principally by caspase-3, because the 32-kDa pro-caspase-3 protein was proteolytically processed in concert with the increase in DEVD-specific cleavage activity. However, we cannot exclude the contribution of caspase-7, which has substrate specificity identical to that of caspase-3, albeit with an approximate 6-fold reduction in cleavage kinetics [51, 52].

The increase in Bax membrane insertion, DEVD-specific cleavage activity and PARP degradation within 8 h of etoposide removal indicates an early commitment to cell death, prior to the detection of G2-arrested cells by flow cytometry. We had predicted that these apoptotic events would be activated either in terminally G2-arrested cells or as they proceeded through an aberrant mitosis to produce multinucleated cells. Instead, over 70% of PARP was degraded at the earliest point of G2 arrest (cf. Figs. 1 and 5). These data indicate either that cell cycle perturbations rapidly signal activation of the apoptotic machinery or that apoptosis is induced independently of cell cycle arrest. It remains to be determined whether the earliest increase in Bax membrane insertion and caspase activity detected (within 8 h of etoposide removal; Fig. 5) is contributed from cells undergoing transient S-phase arrest or from the $<20\%$ of cells that are in the G2 phase at this time.

Overexpression of Bcl-2 in B- and T-cells was recently shown to prevent physiological cell death without affecting cell cycle arrest by interrupting activation of DEVD-specific cleavage activity [15]. Similarly, in this study, overexpression of Bcl-2 in HeLa cells resulted in dissociation of cell cycle arrest and apoptosis, but a high proportion of Bcl-2-expressing cells eventually died through non-apoptotic mechanisms (Fig. 3). That is, etoposide-treated cells undergo cell cycle arrest in the presence of Bcl-2 to an extent similar to that shown by cells that do not overexpress Bcl-2 – without concomitant Bax membrane insertion, an increase in DEVD-specific cleavage activity, or PARP degradation. Therefore, the processes that signal apoptotic events following detection of etoposide-induced DNA damage and/or cell cycle arrest, although ill-defined, are interrupted by Bcl-2 overexpression.

A candidate for an early event in etoposide-induced apoptosis is Bax membrane insertion, with resultant mitochondrial cytochrome c release and activation of caspases [23, 48, 55]. Indeed, Bax movement from the cytosol to membrane fractions occurred within 8 h of etoposide removal in this study. However, the somewhat surprising observation was that Bcl-2 overexpression prevented Bax movement from the cytosol to membrane subcellular fractions despite our expectation that Bax movement would occur upstream of the point at which Bcl-2 acts to interrupt apoptotic events. These data suggest either that Bcl-2 physically blocks the Bax membrane-binding site or that Bcl-2 controls an upstream event necessary for Bax insertion. The mechanism of Bax membrane insertion is currently unknown but is accompanied by a conformational change in the Bax protein [21]. It will be interesting to determine whether this conformational change in Bax occurs in etoposide-treated HeLa cells and, if so, its relationship to Bcl-2 overexpression.

The increased intracellular content of Bcl-2 family member proteins in etoposide-treated S-1 cells deserves comment. First, Bax subcellular redistribution can occur in the absence of its increased expression (that is, Bax membrane insertion was observed as early as at 8 h, whereas increased levels were not detected until 2 days post etoposide treatment). Second, degradation of actin and Bax are late events in the apoptotic cascade (Fig. 4) [3]. Third, changes in individual proteins, except for a moderate (less than 1.5-fold) increase in Bak protein levels, did not occur in the Bcl-2-expressing B-5 cells. Therefore, these changes are unrelated to etoposide-induced cell-cycle arrest and represent sequelae (rather than controlling events) of the apoptotic process. Although we have not determined whether these changes in protein levels occur at the mRNA level, we consider this to be an unlikely scenario and, therefore, unrelated to the p53-induced increase in Bax and Bcl-x_L gene expression observed following DNA damage [27, 58]. A more rational conclusion is that the Bcl-2 members studied are relatively resistant to degradation by caspases and remain intact while other cellular proteins are proteolysed, which, in effect, increases their relative intracellular content. This may reflect their roles in regulating apoptosis. The human Bax protein contains an identical caspase-3 cleavage motif (DELD↓S), present in the D4 G-protein dissociation inhibitor [7], that would be predicted to cleave Bax into approximately 13.7- and 7.5-kDa fragments (similar to the doublet of Bax cleavage fragments detected in Fig. 4A). Interestingly, caspase-3 would be predicted to have a lower cleavage activity against the tetrapeptide DELD than its recognized optimal cleavage sequence DEVD [52], which may explain in part why Bax cleavage is not detected until 4 days following etoposide removal, whereas PARP cleavage is apparent within 8 h (Figs. 4, 5).

The etoposide exposure conditions used in this study caused no apparent difference in the clonogenic survival of S-1 and B-5 cells [35]. However, the clonogenic assay as an indicator of antitumor efficacy has been challenged due to its lack of correlation with in vivo tumor control and to its inability to discriminate cell cycle arrest from

cell death [53]. Therefore, it remained possible in our experiments that Bcl-2 protected cells from etoposide-induced cell death but had not effect on clonogenic survival due to the cell cycle arrest caused by the drug. As mentioned above, long-term experiments did not reveal any greater rate of recovery of Bcl-2-expressing cells following etoposide exposure. Furthermore, these experiments did indicate that Bcl-2-expressing HeLa cells exposed to etoposide eventually lost plasma membrane integrity with little evidence of apoptotic morphology or characteristic DNA degradation. Thus, Bcl-2 may redirect cells from an apoptotic to a necrotic death pathway. In addition, we have demonstrated that Bcl-2 enhances clonogenic survival in an agent-specific fashion in HeLa cells [10]. These data indicate that the therapeutic effects of topoisomerase II poisons may not be affected by apoptosis-specific mechanisms of drug resistance brought about by modulation of Bcl-2 family members.

The etoposide-induced multinucleation phenotype observed in Bcl-2-expressing HeLa cells represents additional rounds of DNA replication in the absence of cell division or apoptosis. This multinucleated phenotype is similar to that observed in the cooperation between Bcl-x_L and loss of p53 to overcome a mitotic spindle checkpoint [42]. A notable exception is that etoposide treatment results in the formation of additional small nuclear fragments, probably as a result of reformation of the nuclear membrane around acentric chromosomal fragments caused by topoisomerase II-mediated DNA cleavage [35]. It has recently been shown that p53 prevents proliferation and induces apoptosis in micronucleated cells [49, 50] and that pRb is necessary to prevent DNA re-replication in the absence of cell division [45]. HeLa cells lack functional p53 and pRb checkpoints due to human papillomavirus infection [4, 16, 19].

The precise mechanism of etoposide-induced apoptosis in non-Bcl-2-expressing HeLa (S-1) cells remains unknown. However, it is unlikely to be due to reactivation of p53, as concomitant G-1 arrest would be expected to occur via $p21^{Cip/Waf1}$ induction [9]. This possibility cannot be excluded, however, as high concentrations of genotoxic agents have been observed to interrupt expression of the HPV E6 and E7 proteins [5]. Nevertheless, we have observed $p21^{Cip1/Waf1}$ induction only using supralethal etoposide exposure conditions, not under the conditions used in this study [37]. Despite a minor proportion of non-apoptotic S-1 cells appearing with $>4n$ DNA content following etoposide exposure (around 20%; Fig. 2B, region 2, Fig. 3A), clearly a higher proportion of apoptotic cells contain $>4n$ DNA content (Fig. 2B, region 3). These data suggest that despite the early activation of DEVD-specific cleavage activity, Bax membrane insertion and PARP degradation, the majority of etoposide-treated S-1 cells become multinucleated but then rapidly undergo apoptosis (as measured by DNA degradation; Figs. 2B, 3A). Whatever the mechanism(s) of apoptosis induction in etoposide-treated HeLa cells, it is inhibited by Bcl-2 overexpression, which then appears to allow DNA re-replication in the absence of cell division, probably due to the lack of functional p53 and pRb checkpoints.

In summary, Bcl-2 overexpression in HeLa cells does not affect etoposide-induced cell-cycle arrest but instead interrupts the apoptosis signaling cascade. Prevention of Bax membrane insertion, caspase activation and PARP cleavage, presumably along with additional apoptotic events not assayed in this study, results in cells that are either terminally G2-arrested or undergo rounds of DNA re-replication in the absence of cell division. This eventually leads to loss of plasma membrane integrity without the morphological changes or DNA degradation characteristic of apoptosis. It will be interesting to determine whether Bcl-2, by delaying etoposide-induced cell death, causes an increase in rates of gene mutation that might also contribute to resistance to chemotherapeutic drugs.

Acknowledgements This work was supported by RPG-98-063-CCE from the American Cancer Society, the Henry Vogt Cancer Research Institute, the Regional Cancer Center Corporation of the J. Graham Brown Cancer Center, and by the Children's Cancer Research Institute. Kathleen M. Murphy was supported in part by a grant from the DEPSCoR initiative in Kentucky to Dr. Uldis N. Streips. The contents of this report are solely the responsibility of the authors and do not necessarily represent the official views of the funding agencies.

References

1. Bedi A, Barber JP, Bedi GC, Eldeiry WS, Sidransky D, Vala MS, Akhtar AJ, Hilton J, Jones RJ (1995) BCR-ABL-mediated inhibition of apoptosis with delay of G2/M transition after DNA damage: a mechanism of resistance to multiple anticancer agents. Blood 86: 1148
2. Bossy-Wetzel E, Newmayer DD, Green DR (1998) Mitochondrial cytochrome c release in apoptosis occurs upstream of DEVD-specific caspase activation and independently of mitochondrial transmembrane depolarization. EMBO J 17: 37
3. Brown SB, Bailey K, Savill J (1997) Actin is cleaved during constitutive apoptosis. Biochem J 323: 233
4. Butz K, Shahabeddin L, Geisen C, Spitkovsky D, Ullmann A, Hoppe-Seyler F (1995) Functional p53 protein in human papillomavirus-positive cancer cells. Oncogene 10: 927
5. Butz K, Geisen C, Ullmann A, Spitkovsky D, Hoppe-Seyler F (1996) Cellular responses of HPV-positive cancer cells to genotoxic anti-cancer agents: repression of E6/E7-oncogene expression and induction of apoptosis. Int J Cancer 68: 506
6. Chen AY, Liu LF (1994) DNA topoisomerases: essential enzymes and lethal tagets. Annu Rev Pharmacol Toxicol 34: 191
7. Cohen GM (1997) Caspases: the executioners of apoptosis. Biochem J 326: 1
8. Drewinko B, Barlogie B (1976) Survival and cycle-progression delay of human lymphoma cells in vitro exposed to VP-16-213. Cancer Treat Rep 60: 1295
9. El-Deiry WS, Harper JW, O'Connor PM, Velculescu VE, Canman CE, Jackman J, Pietenpol JA, Burrell M, Hill DE, Wang Y, Wilman KG, Mercer WE, Kastan MB, Kohn KW, Elledge SJ, Kinzler KW, Vogelstein B (1994) *WAF1/CIP1* is inducted in *p53*-mediated G_1 arrest and apoptosis. Cancer Res 54: 1169
10. Elliott MJ, Stribinskiene L, Lock RB (1998) Expression of Bcl-2 in human epithelial tumor (HeLa) cells enhances clonogenic survival following exposure to 5-fluoro-2′-deoxyuridine or

staurosporine, but not following exposure to etoposide or doxorubicin. Cancer Chemother Pharmacol 41: 457
11. Emoto Y, Kisaki H, Manome Y, Kharbanda S, Kufe D (1996) Activation of protein kinase C δ in human myeloid leukemia cells treated with 1-β-D-arabinofuranosylcytosine. Blood 87: 1990
12. Erhardt P, Cooper GM (1996) Activation of the CPP32 apoptotic protease by distinct signaling pathways with differential sensitivity to bcl-x(L). J Bio Chem 271: 17601
13. Fraser A, Evan G (1996) A license to kill. Cell 85: 781
14. Gorczyca W, Gong J, Darzynkiewicz Z (1993) Detection of DNA strand breaks in individual apoptotic cells by the in situ terminal deoxynucleotidyl transferase and nick translation assays. Cancer Res 53: 1945
15. Harvey KJ, Blomquist JF, Ucker DS (1998) Commitment and effector phases of the physiological cell death pathway elucidated with respect to Bcl-2, caspase, and cyclin-dependent kinase activities. Mol Cell Biol 18: 2912
16. Hickman ES, Picksley SM, Vousden KH (1994) Cells expressing HPV16 E7 continue cell cycle progression following DNA damage induced p53 activation. Oncogene 9: 2177
17. Hickman JA (1992) Apoptosis induced by anticancer drugs. Cancer Metastasis Rev 11: 121
18. Hickman JA (1996) Apoptosis and chemotherapy resistance. Eur J Cancer 32A: 921
19. Hoppe-Seyler F, Butz K (1993) Repression of endogenous p53 transactivation function in HeLa cervical carcinoma cells by human papillomavirus type 16 E6, human mdm-2, and mutant p53. J Virol 67: 3111
20. Hsu Y-T, Youle RJ (1997) Nonionic detergents induce dimerization among members of the Bcl-2 family. J Biol Chem 272: 13829
21. Hsu Y-T, Youle RJ (1998) Bax in murine thymus is a soluble monomeric protein that displays differential detergent-induced conformations. J Biol Chem 273: 10777
22. Hsu Y-T, Wolter KG, Youle RJ (1997) Cytosol-to-membrane redistribution of Bax and Bcl-X(L) during apoptosis. Proc Natl Acad Sci USA 94: 3668
23. Jurgensmeier JM, Xie Z, Deveraux Q, Ellerby L, Bredesen D, Reed JC (1998) Bax directly induces release of cytochrome c from isolated mitochondria. Proc Natl Acad Sci USA 95: 4997
24. Kaufmann SH, Desnoyers S, Ottaviano Y, Davidson NE, Poirier GG (1993) Specific proteolytic cleavage of poly(ADP-ribose) polymerase: an early marker of chemotherapy-induced apoptosis. Cancer Res 53: 3976
25. Kerr JFR, Wyllie AH, Currie AR (1972) Apoptosis: a basic biological phenomenon with wide-ranging implications in tissue kinetics. Br J Cancer 26: 239
26. Kerr JFR, Winterford CM, Harmon BV (1994) Apoptosis: its significance in cancer and cancer therapy. Cancer 73: 2013
27. Kitada S, Krajewski S, Miyashita T, Krajewska M, Reed JC (1996) γ-Radiation induces upregulation of Bax protein and apoptosis in radiosensitive cells in vivo. Oncogene 12: 187
28. Kluck RM, Bossy-Wetzel E, Green DR, Newmeyer DD (1997) The release of cytochrome c from mitochondria: a primary site for Bcl-2 regulation of apoptosis. Science 275: 1132
29. Kroemer G (1997) The proto-oncogene Bcl-2 and its role in regulating apoptosis. Nature Med 3: 614
30. Lazebnik YA, Kaufmann SH, Desnoyers S, Poirier GG, Earnshaw WC (1994) Cleavage of poly(ADP-ribose) polymerase by a proteinase with properties like ICE. Nature 371: 346
31. Li P, Nijhawan D, Budihardjo I, Srinivasula SM, Ahmad M, Alnemri ES, Wang X (1997) Cytochrome c and dATP-dependent formation of Apaf-1/caspase-9 complex initiates an apoptosis protease cascade. Cell 91: 479
32. Lock RB (1992) Inhibition of $p34^{cdc2}$ kinase activation, $p34^{cdc2}$ tyrosine dephosphorylation, and mitotic progression in Chinese hamster ovary cells exposed to etoposide. Cancer Res 52: 1817
33. Lock RB, Keeling PK (1993) Responses of HeLa and Chinese hamster ovary $p34^{cdc2}$/cyclin-B kinase in relation to cell cycle perturbations induced by etoposide. Int J Oncol 3: 33
34. Lock RB, Ross WE (1990) Inhibition of $p34^{cdc2}$ kinase activity by etoposide or irradiation as a mechanism of G_2 arrest in Chinese hamster ovary cells. Cancer Res 50: 3761
35. Lock RB, Stribinskiene L (1996) Dual modes of death induced by etoposide in human epithelial tumor cells allow Bcl-2 to inhibit apoptosis without affecting clonogenic survival. Cancer Res 56: 4006
36. Lock RB, Galperina OV, Feldhoff RC, Rhodes LJ (1994) Concentration-dependent differences in the mechanisms by which caffeine potentiates etoposide cytotoxicity in HeLa cells. Cancer Res 54: 4933
37. Lock RB, Thompson BS, Sullivan DM, Stribinskiene L (1997) Potentiation of etoposide-induced apoptosis by staurosporine in human tumor cells is associated with events downstream of DNA-protein complex formation. Cancer Chemother Pharmacol 39: 399
38. Lowe SW, Bodis S, McClatchey A, Remington L, Ruley HE, Fisher DE, Housman DE, Jacks T (1994) *p53* Status and the efficacy of cancer therapy in vivo. Science 266: 807
39. Martin SJ, Green DR (1995) Protease activation during apoptosios: death by a thousand cuts? Cell 82: 349
40. Martins LM, Kottke T, Mesner PW, Basi GS, Sinha S, Frigon N, Tatar E, Tung JS, Bryant K, Takahashi A, Svingen PA, Madden BJ, McCormick DJ, Earnshaw WC, Kaufmann SH (1997) Activation of multiple interleukin-1 beta converting enzyme homologues in cytosol and nuclei of HL-60 cells during etoposide-induced apoptosis. J Biol Chem 272: 7421
41. Martins LM, Mesner PW, Kottke TJ, Basi GS, Sinha S, Tung JS, Svingen PA, Madden BJ, Takahashi A, McCormick DJ, Earnshaw WC, Kaufmann SH (1997) Comparison of caspase activation and subcellular localization in HL-60 and K562 cells undergoing etoposide-induced apoptosis. Blood 90: 4283
42. Minn AJ, Boise LH, Thompson CB (1996) Expression of bcl-x(L) and loss of p53 can cooperate to overcome a cell cycle checkpoint induced by mitotic spindle damage. Genes Dev 10: 2621
43. Morana SJ, Wolf CM, Li JF, Reynolds JE, Brown MK, Eastman A (1996) The invovlement of protein phosphatases in the activation of ICE/CED-3 protease, intracellular acidification, DNA digestion, and apoptosis. J Biol Chem 271: 18263
44. Nicholson DW, Ali A, Thornberry NA, Vaillancourt JP, Ding CK, Gallant M, Gareau Y, Griffin PR, Labelle M, Lazebnik YA, Munday NA, Raju SM, Smulson ME, Yamin T-T, Yu VL , Miller DK (1995) Identification and inhibition of the ICE/CED-3 protease necessary for mammalian apoptosis. Nature 376: 37
45. Niculescu AB III, Chen X, Smeets M, Hengst L, Prives C, Reed IS (1998) Effects of $p21^{Cip1/Waf1}$ at both the G_1/S and the G_2/M cell cycle transitions: pRb is a critical determinant in blocking DNA replication and in preventing endoreduplication. Mol Cell Biol 18: 629
46. Reed JC, Miyashita T, Takayama S, Wang HG, Sato T, Krajewski S, Aimesempe C, Bodrug S, Kitada S, Hanada M (1996) BCL-2 family proteins: regulators of cell death involved in the pathogenesis of cancer and resistance to therapy. J Cell Biochem 60: 23
47. Rosen A, Casciola-Rosen L (1997) Macromolecular substrates for the ICE-like proteases during apoptosis. J Cell Biochem 64: 50
48. Rosse T, Olivier R, Monney L, Rager M, Conus S, Fellay I, Jansen B, Borner C (1998) Bcl-2 prolongs cell survival after Bax-induced release of cytochrome c. Nature 391: 496
49. Sablina AA, Ilyinskaya GV, Rubtsova SN, Agapova LS, Chumakov PM, Kopnin BP (1998) Activation of p53-mediated cell cycle checkpoint in response to micronuclei formation. J Cell Sci 111: 977
50. Schwartz D, Almog A, Peled A, Goldfinger N, Rotter V (1997) Role of wild type p53 in the G_2 phase: regulation of the γ-irradiation-induced delay and DNA repair. Oncogene 15: 2597
51. Talanian RV, Quinlan C, Trautz S, Hackett MC, Mankovich JA, Banach D, Ghayur T, Brady KD, Wong WW (1997)

Substrate specificities of caspase family proteases. J Biol Chem 272: 9677
52. Thornberry NA, Rano TA, Peterson EP, Rasper DM, Timkey T, Garcia-Calvo M, Houtzager VM, Nordstrom PA, Roy S, Vaillancourt JP, Chapman KT, Nicholson DW (1997) A combinatorial approach defines specificities of members of the caspase family and granzyme B. J Biol Chem 272: 17907
53. Waldman T, Zhang Y, Dillehay L, Yu J, Kinzler K, Vogelstein B, Williams J (1997) Cell-cycle arrest versus cell death in cancer therapy. Nature Med 3: 1034
54. Wolf CM, Reynolds JE, Morana SJ, Eastman A (1997) The temporal relationship between protein phosphatase, ICE/CED-3 proteases, intracellular acidification, and DNA fragmentation in apoptosis. Exp Cell Res 230: 22
55. Wolter KG, Hsu YT, Smith CL, Nechushtan A, Xi X-G, Youle RJ (1997) Movement of Bax from the cytosol to mitochondria during apoptosis. J Cell Biol 139: 1281
56. Yang E, Korsmeyer SJ (1996) Molecular thanatopsis: a discourse on the Bcl2 family and cell death. Blood 88: 386
57. Yang J, Liu X, Bhalla K, Kim CN, Ibrado AM, Cai J, Peng T-1, Jones DP, Wang X (1997) Prevention of apoptosis by Bcl-2: release of cytochrome c from mitochondria blocked. Science 275: 1129
58. Zhan QM, Alamo I, Yu K, Boise LH, Cherney B, Tosato G, O'Connor PM, Fomace AJ (1996) The apoptosis-associated gamma-ray response of BCL-X(L) depends on normal p53 function. Oncogene 13: 2287